Agricultural and Forest Meteorology 149 (2009) 1907–1918

Contents lists available at ScienceDirect

Agricultural and Forest Meteorology

journal homepage: www.elsevier.com/locate/agrformet

Refinement of rooting depths using satellite-based evapotranspiration seasonality for ecosystem modeling in California

Kazuhito Ichii [a,b,*], Weile Wang [b,c], Hirofumi Hashimoto [b,c], Feihua Yang [d], Petr Votava [b,c], Andrew R. Michaelis [b,c], Ramakrishna R. Nemani [b]

[a] Faculty of Symbiotic Systems Science, Fukushima University, 1 Kanayagawa, Fukushima, 960-1296, Japan
[b] NASA Ames Research Center, Moffett Field, CA, USA
[c] University Corporation at Monterey Bay, Seaside, CA, USA
[d] Department of Geography, University of Wisconsin, Madison, WI, USA

ARTICLE INFO

Article history:
Received 28 October 2008
Received in revised form 22 June 2009
Accepted 25 June 2009

Keywords:
Terrestrial ecosystem modeling
Water cycle
Carbon cycle
Remote sensing
Regional modeling
Rooting depth

ABSTRACT

Accurate determination of rooting depths in terrestrial biosphere models is important for simulating terrestrial water and carbon cycles. In this study, we developed a method for optimizing rooting depth using satellite-based evapotranspiration (ET) seasonality and an ecosystem model by minimizing the differences between satellite-based and simulated ET. We then analyzed the impacts of rooting depth optimization on the simulated ET and gross primary production (GPP) seasonality in California, USA. First, we conducted a point-based evaluation of the methods against flux observations in California and tested the sensitivities of the simulated ET seasonality to the rooting depth settings. We then extended it spatially by estimating spatial patterns of rooting depth and analyzing the sensitivities of the simulated ET and GPP seasonalities to the rooting depth settings. We found large differences in the optimized and soil survey (STATSGO)-based rooting depths over the northern forest regions. In these regions, the deep rooting depths (>3 m) estimated in the study successfully reproduced the satellite-based ET seasonality, which peaks in summer, whereas the STATSGO-based rooting depth (<1.5 m) failed to sustain a high ET in summer. The rooting depth refinement also has large effects on simulated GPP; the annual GPP in these regions is increased by 50–100% due to sufficient soil water during the summer. In the grassy and shrubby regions of central and southern California, the estimated rooting depths are similar to those of STATSGO, probably due to the shallow rooting depth in these ecosystems. Our analysis suggests that setting a rooting depth is important for terrestrial ecosystem modeling and that satellite-based data could help both to estimate the spatial variability of rooting depths and to improve water and carbon cycle modeling.

1. Introduction

Accurate modeling of the soil water balance and evapotranspiration is essential for analyzing hydrological processes, water management, and carbon cycles in terrestrial environments. Soil water balance, which is determined by various water cycle processes, such as precipitation, snowfall, snowmelt, evaporation, transpiration, infiltration, and runoff, influences precipitation, temperature, and atmospheric circulation through the release of latent heat flux (e.g., Koster et al., 2004; Huang et al., 1996). Photosynthesis and heterotrophic respiration are also affected by soil water availabilities through stomatal conductance closure (e.g., Ball et al., 1987) and water availability for microbes (e.g., Andren and Paustian, 1987), which, in turn, affects the terrestrial carbon budget (e.g., Nemani et al., 2002). The accuracy of soil water simulations also impacts climate forecasting capabilities (e.g., Huang et al., 1996; Yang et al., 2004; Alfaro et al., 2006).

Because evapotranspiration (ET) is a major component of the terrestrial water and energy cycles, its accurate modeling is essential for soil water modeling. The accuracy largely depends on model structure and parameters (Guswa et al., 2002), meteorological data (e.g., White and Nemani, 2004; Rawlins et al., 2006), vegetation phenology (e.g., White and Nemani, 2004; Buermann et al., 2001), and below-ground properties (e.g., soil texture and rooting depth) (Lathrop et al., 1995; Kleidon and Heimann, 1998). Among model-related properties (model structure, ecophysiological parameters and below-ground properties), evaluation of rooting depth is essential because it is the primary determinant of

* Corresponding author at: Faculty of Symbiotic Systems Science, Fukushima University, 1 Kanayagawa, Fukushima, 960-1296, Japan. Tel.: +81 24 548 5256; fax: +81 24 548 5256.
E-mail address: kazuhito.ichii@gmail.com (K. Ichii).

0168-1923/$ – see front matter © 2009 Elsevier B.V. All rights reserved.
doi:10.1016/j.agrformet.2009.06.019

the maximum plant available water in the rooting zone and it affects vegetation productivity through water stress during the dry season. Generally, model-related properties which control evapotranspiration and soil water content include maximum stomatal conductance, limiting functions of stomatal conductance to environment variables, soil texture, and rooting depth. Maximum conductance determines magnitude of seasonal ET variations and its peak, limiting functions of stomatal conductance regulate ET due to severe environmental condition, soil texture determines volumetric water content, and only rooting depth substantially determines amount of plant available water in the vertical soil layer.

Although rooting depth can be determined via soil surveys, several studies have pointed out that soil survey-based values underestimate the true depth because direct observation of rooting depth is not available for many regions, and only a small portion of direct observations (<10%) reached to maximum rooting depth (Schenk and Jackson, 2002). A small number of deep roots could have a significant role in water uptake in dry seasons. Indeed, default rooting depth settings in many ecosystem models are shallow (usually <2 m; e.g. 1.5 m for LPJ model; Sitch et al., 2003, 1.0 m for CASA model; Potter et al., 1993), and some studies have highlighted the existence of deep rooting systems in seasonally water-limited ecosystems (e.g., Nepstad et al., 1994; Canadell et al., 1996; Schenk and Jackson, 2002, 2005) and the importance of their inclusion in models for the accurate simulation of the carbon and water cycles (Kleidon and Heimann, 1998; Tanaka et al., 2004; Ichii et al., 2007; Baker et al., 2008). Several studies have inferred rooting depth by finding the depth that achieves maximum net primary productivity (NPP) (Kleidon and Heimann, 1998) or that maximizes the correlation of modeled GPP and the satellite-based vegetation index seasonality (Ichii et al., 2007). However, none of these studies used actual observations (e.g., observed ET) to determine rooting depth.

Another difficulty with soil water and evapotranspiration modeling is the lack of sufficient observations to provide the information necessary to constrain the model parameters (e.g., Zhu and Liang, 2005). However, recent advances in satellite observations provide an opportunity to monitor spatio-temporal patterns in terrestrial water cycles, enabling spatial patterns of ET to be obtained with sufficient accuracy (e.g., Nishida et al., 2003; Yang et al., 2006; Zhang and Wegehenkel, 2006). These seasonal variations have the potential to be used to constrain the model.

The purpose of this study is to refine the rooting depth data in the terrestrial biosphere model using satellite-based ET seasonality to improve the modeling capability for simulating both water and carbon cycle seasonalities in California. We used the Terrestrial Observation and Prediction System (TOPS) (Nemani et al., 2003) as an ecosystem model and we used a support vector machine (SVM)-based ET estimation (Yang et al., 2006) as a satellite-based ET. First, TOPS was used to estimate rooting depths, and we tested the sensitivities of the simulated ET seasonality to the rooting depth settings at flux sites in California. The analysis was then extended spatially, and we analyzed the sensitivities of the simulated ET and GPP seasonalities to the rooting depth setting.

2. Data and method

2.1. Study area

We focused our analysis on California, USA (Fig. 1). California is mostly characterized by a Mediterranean climate with a dry season in summer (e.g., April–September and March–October in the northern and southern regions, respectively) and a wet season in winter (e.g., December–February) (Fig. 2). Land cover patterns

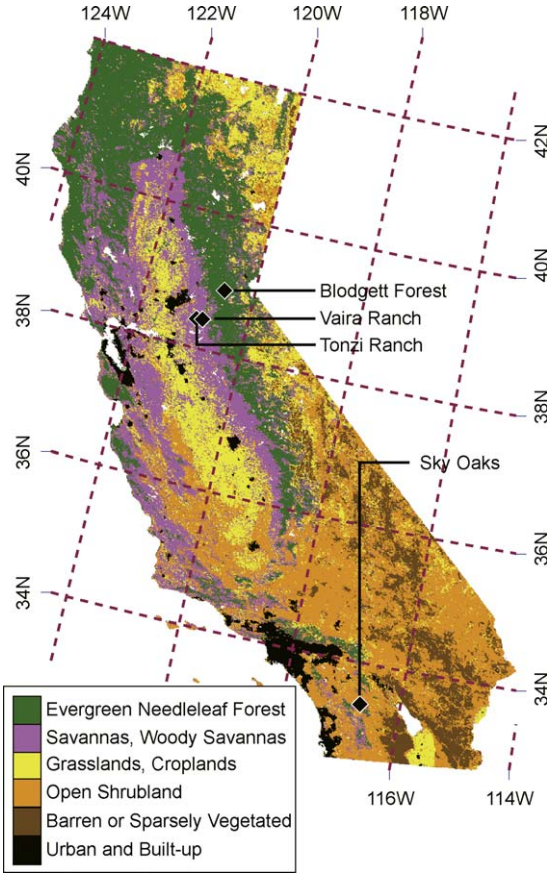

Fig. 1. Land cover of the study area with flux observation sites in California based on MODIS land cover data (MOD12Q1; Friedl et al., 2002) in the year 2001. Diamonds (◆) show the locations of flux observation stations used in the study.

follow the precipitation patterns, with evergreen needle-leaf forests over northern California in the high-precipitation regions, cropland and Savanna in the central valley, and open shrubland that has little precipitation in the southern regions. The middle to southern coastal regions are characterized by higher precipitation than the inland areas.

2.2. Models

2.2.1. Satellite data-based ET

We used a machine learning technique for regressions to obtain spatio-temporal ET variations as described by Yang et al. (2006). The method is based on the regression-type support vector machine (SVM), which transforms a non-linear regression into a linear regression by mapping the original low-dimensional input space to a higher dimensional feature space using kernel functions (e.g., Vapnik, 1998; Cristianini and Shawe-Taylor, 2000), with inputs of satellite-based incoming surface solar radiation (Rad), land surface temperature (LST), enhanced vegetation index (EVI), and land cover (Yang et al., 2006). The method was assessed at more than 20 Ameriflux sites over the continental United States, and the method was extended spatially using satellite data. The method was determined to be effective for predicting spatio-temporal ET patterns with acceptable accuracy (e.g., $R^2 = 0.75$ and root mean square error (RMSE) = 0.62 mmH_2O day^{-1}; Yang et al., 2006).

The SVM analysis consists of three main steps for model tuning and testing. First, the SVM model parameters (C: cost of errors, ε: width of an insensitive error band, and σ: kernel parameter) were obtained from a training set. Second, with the obtained parameters

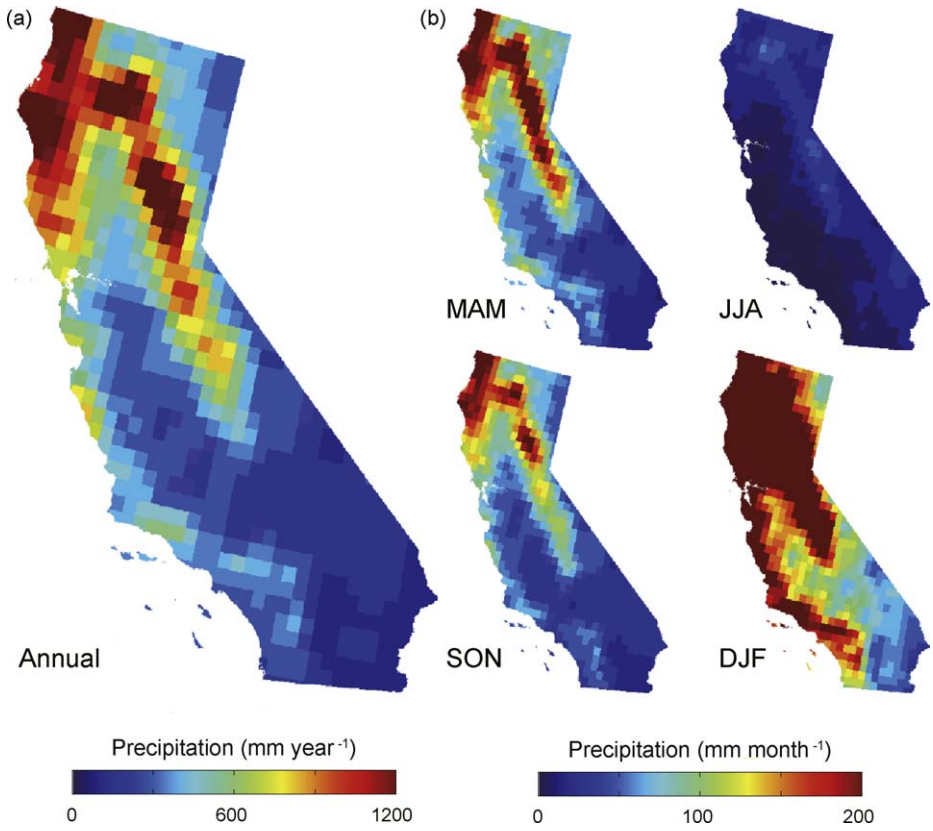

Fig. 2. (a) Annual and (b) seasonal patterns of precipitation based on US daily precipitation real-time analysis from the Climate Prediction Center, averaged over 2001–2006. MAM, JJA, SON, and DJF denote March–May, June–August, September–November, and December–February, respectively.

for the model structure, we trained the model. Last, we evaluated the model based on a test set. More details regarding the methods are described by Yang et al. (2006). After evaluation, the model was employed to obtain spatio-temporal variations of ET in California using satellite-based data. 8-day ET averages were estimated for both point and spatial analyses in every experiment. The data used for the SVM model came from flux sites in the western United States (Table 1 and Section 2.3.1).

2.2.2. Terrestrial water/carbon cycle model

We used TOPS to simulate the daily water and carbon cycle processes (Nemani et al., 2003, 2009; White and Nemani, 2004). TOPS integrates satellite data, ecosystem modeling, and static land cover and soil information to simulate ecosystem status. Simulations of hydrologic states and fluxes are based largely on the Biome-BGC model (Thornton, 1998; Thornton et al., 2002) with the use of the remotely sensed leaf area index (LAI). Calculation of GPP is based on a production efficiency model (PEM) approach. Here, we provide a summary of the water cycle and GPP models in TOPS; details are described by White and Nemani (2004) and Ichii et al. (2008).

Daily water budgets are calculated as the net flux of rainfall, snowfall, evapotranspiration (ET is the sum of transpiration, soil evaporation, canopy water evaporation, and snow sublimation), snowmelt, and runoff. The snow model draws from a physically based energy balance model (Ichii et al., 2008). ET is calculated based on a Penman–Monteith approach using LAI and meteorology. Stomatal conductance, the primary determinant of transpiration, is formulated empirically (the Stewart adaptation of the Jarvis model; Stewart, 1988) with maximum stomatal conductance and temperature, vapor pressure deficit (VPD), radiation, and soil water limitation factors. Soil water content affects stomatal conductance through changes in leaf water potential and is expressed as the balance between the inputs (snowmelt and precipitation) and outputs (ET and runoff). Base-flow runoff component is not included in the model and soil water in excess of the soil water holding capacity is routed to runoff.

Table 1
Flux sites used in this study.

Site name	State	Longitude	Latitude	Veg. class	References
Blodgett Forest	CA	−120.6328	38.8953	ENF	Goldstein et al. (2000) Misson et al. (2006)
Vaira Ranch	CA	−120.9507	38.4067	SV	Baldocchi et al. (2004)
Tonzi Ranch	CA	−120.996	38.4316	SV	Baldocchi et al. (2004)
Sky Oaks Young Stand	CA	−116.623	33.3772	SH	Stylinski et al. (2002)
Sky Oaks Old Stand	CA	−116.623	33.3739	SH	Stylinski et al. (2002)
Sky Oaks	CA	−116.640	33.3844	SH	Lipson et al. (2005)
Audubon grasslands	AZ	−110.5104	31.6000	GR	–
Metolius old ponderosa pine	OR	−121.6224	44.4992	ENF	Law et al. (2004)
Metolius first young aged pine	OR	−121.5668	44.4372	ENF	Law et al. (2004)
Wind River	WA	−121.9519	45.8205	ENF	Shaw et al. (2004)

Abbreviations of vegetation classes: evergreen needle-leaf forest (ENF), Savanna (SV), Shrubland (SH), and Grassland (GR).

Table 2
Ecophysiological parameters for TOPS model used in this study.

Parameter	Unit	ENF	SV	GR/CR	SH
Maximum stomatal conductance	mm s^{-1}	0.002	0.002	0.002	0.0012
VPD: start of conductance reduction	Pa	600	600	600	600
VPD: end of conductance reduction	Pa	3000	3000	3000	3000
LWP: start of conductance reduction	MPa	−0.1	−0.1	−0.1	−0.1
LWP: end of conductance reduction	MPa	−1.5	−1.5	−1.5	−1.5
Canopy water interception coefficient	Fraction LAI^{-1}	0.001	0.001	0.001	0.001

Abbreviations of parameters: vapor pressure deficit (VPD) and leaf water potential (LWP). Abbreviations of vegetation classes: cropland (CR).

Daily GPP is calculated based on a PEM approach (e.g., Monteith, 1972):

$$\mathrm{GPP} = \varepsilon_{\max} \cdot \mathrm{APAR} \cdot f(\mathrm{environment}) \quad (1)$$

where $\varepsilon_{\max}$ is the maximum light use efficiency, APAR is the absorbed photosynthetically active radiation, calculated as the product of photosynthetically active radiation (PAR) and FPAR (the fraction of PAR absorbed by plant canopies), and f(environment) is an environmental stress scalar set as the minimum limitation of daily minimum temperature, VPD, and soil water. The environmental stress scalar in each limitation factor ranges linearly from 0 (total inhibition of photosynthesis) to 1 (no inhibition) and is defined in the same way as the stomatal conductance modeling.

We changed the formulations of soil water effects on stomatal conductance and GPP in this study. Although the original model used the soil water potential converted from the volumetric water content in the soil layer to reduce the stomatal conductance and GPP, we used the volumetric water content instead. This modification slightly improved the RMSEs between the modeled and satellite-based ET seasonality. The volumetric water contents that correspond to the wilting point of soil (−1.5 MPa) and the start of conductance closure (set as −0.1 MPa; Table 2) are used to linearly reduce stomatal conductance as a water stress.

We briefly describe the effects of rooting depth on ET and GPP in the model. The setting of the rooting depth determines the vertical extent of the soil water storage accessible to plants; i.e., a deep rooting depth increases the soil water holding capacity. Soil water content is calculated by the water balance of precipitation, snowmelt, evapotranspiration, and runoff, and the soil water holding capacity is used to calculate runoff; i.e., soil water in excess of the soil water holding capacity is routed to runoff. Therefore, soils with high water-holding capacities can store more water in the wet season and, in turn, sustain photosynthesis and evapotranspiration during the dry season (Fig. 3(a)). On the other hand, soils with shallow rooting depths cannot hold enough water to sustain photosynthesis and evapotranspiration during the dry season, which leads to soil water stress, stomatal closure, and ET and GPP reduction (Fig. 3(b)).

Ecophysiological parameters for each plant functional type are derived from Biome-BGC values (White et al., 2000). We made some changes to these parameters (Table 2) by comparing the observed ET data to adjust the maximum stomatal conductance and canopy leaf interception parameters, because simulations based on the default parameters caused an overestimation of evapotranspiration.

2.2.3. Rooting depth determination

We used satellite-based ET seasonality and the TOPS terrestrial biosphere model to infer the suitable rooting depth for the TOPS simulation at each grid. Because rooting depth potentially affects ET seasonality during the dry season (see Section 2.2.2), we can inversely estimate rooting depth using ET seasonality. For example, if the observed ET is high during the dry season, the

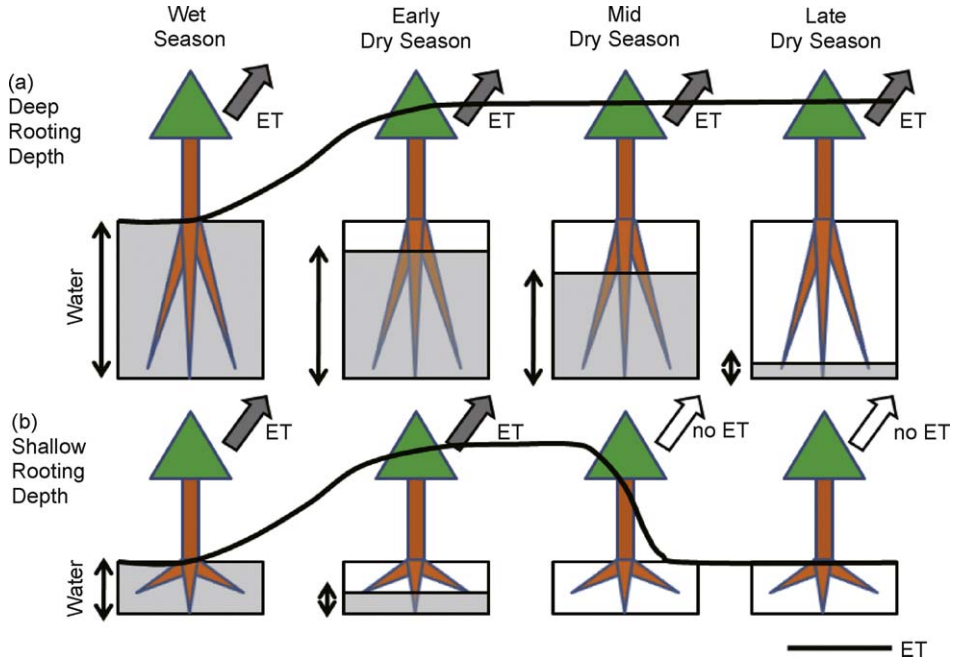

Fig. 3. Conceptual image of the method of determining rooting depth. (a) In the region with a long dry season, vegetation utilizes the water stored in the wet season. (b) In the case of a shallow rooting depth setting, soil water is dried out in the mid and end dry seasons, which suppresses evapotranspiration and gross primary production. In the case of deep rooting depth, stored water in the wet season can sustain the vegetation growth throughout the entire dry season.

ecosystem must have a deep rooting system to supply soil water in the absence of rainfall (Fig. 3(a)). Conversely, if the observed ET is diminished in the dry season, the ecosystem has a certain level of rooting depth (Fig. 3(b)).

To find the appropriate rooting depth for the model, we used the Golden Section Search algorithm (Press et al., 1992) as one-dimensional optimization problem to minimize the RMSE between the observed and simulated ETs (e.g., Kleidon and Heimann, 1998; Kleidon, 2004). Initially, we set the range of rooting depth from 0.1 to 10.0 m and executed until the algorithm found the rooting depth that minimizes the RMSE between the satellite-based and simulated ETs, using every 8-day ET variation from 2001 to 2003. In this simulation, we found that, above a certain level of rooting depth, there is very little sensitivity to the seasonal ET variation in virtually no water stressed vegetation because there is enough available water to sustain vegetation growth in the dry season. Therefore, we set a standard to find the minimum rooting depth that does not impart any additional change in the model accuracy (RMSE) (<1%). We repeated this 30 times, until the rooting depth values converged.

2.3. Data

We used (1) flux tower observation data, (2) satellite-based data, (3) meteorological data, and (4) static data. Table 3 lists the data used in the study and their purposes.

2.3.1. Flux tower observation data

We used flux tower observation data from 2000 to 2006, from 10 sites over the western United States (Table 1). The sites are located throughout California, Arizona, Oregon, and Washington. We obtained the Level 4 (gap-filled) weekly (8-day) ET and surface radiation observations from the Ameriflux website (http://public.ornl.gov/ameriflux). These data are used for (1) satellite data-based ET estimation (ET and Rad) and (2) model validation (ET). We obtained 1173 observation dates, including 435 for forest sites and 738 for non-forest sites.

2.3.2. Satellite-based time-variable data

We used an 8-day composite of the Moderate Resolution Imaging Spectroradiometer (MODIS)-based LST (Wan et al., 2002) and EVI (Huete et al., 2002) for the satellite-based ET estimation and FPAR/LAI (Myneni et al., 2002) for the TOPS model from 2000 to 2006 (Collection 4 data). The EVI is originally composited on a 16-day basis; we therefore assigned each 16-day composite EVI to its two corresponding 8-day periods. For the satellite-based ET evaluation processes at the flux sites, we used MODIS 1-km resolution American Standard Code for Information Interchange (ASCII) subset data sets, each of which consisted of 7 by 7 km regions centered on the flux towers for LST and EVI (Cook et al., 2004). At each time step, we averaged these values using the high-quality pixels (with the mandatory quality assurance (QA) flag being good in the QA data). If none of the 49 values was of high enough quality, we treated the period as missing. For the flux-site model evaluation processes, we used the LAI and FPAR (for the TOPS model) and LST and EVI (for satellite-based ET estimation) from the MODIS 1-km ASCII subset data, and missing data were replaced by a 2001–2006 average calculated from high-quality pixels. For the spatial analysis, we used original 1-km spatial resolution data from MODIS LST and EVI for satellite-based ET estimation and FPAR/LAI for TOPS inputs; for data cleaning, all data were filled using averaged 8-day data calculated from 2001 to 2006 at each grid point if the QA flags were not good.

2.3.3. Meteorological data

We used daily gridded climate data from 1996 to 2006 for the analysis. Daily maximum and minimum temperatures were produced by kriging with altitude correction, using point observations from the National Climatic Data Center (NCDC) data (Jolly et al., 2005). Vapor pressure deficit (VPD) was calculated by assigning the daily minimum temperature as the dew point temperature (Campbell and Norman, 1998). Daily precipitation fields are derived from real-time analysis of U.S. daily precipitation by the Climate Prediction Center at quarter degree resolution (available at http://www.cpc.ncep.noaa.gov/products/precip/realtime/retro.shtml). Radiation data are from the Surface Radiation Budget (SRB, derived from the Geostationary Operational Environmental Satellite and original spatial resolution is 0.25 degree) project, which relies on satellite observations and on an atmospheric radiative transfer model (Pinker et al., 2002). Missing radiation values were filled by long-term means. We used the 8-day average of radiation as an input for the satellite-based ET estimation and all daily climate fields as TOPS model inputs.

2.3.4. Static data

The static data consist of land cover, soil properties, and elevation. Land cover data are derived from MODIS Land Cover data (MOD12Q1; Friedl et al., 2002) and are used as inputs for the satellite-based ET estimation and TOPS. Using a data set of 1-km gridded soils from Pennsylvania State University (based on the State Soil Geographic Database, STATSGO, and created by Miller and White, 1998), we generated soil depth and percent sand, silt, and clay, as required by TOPS. For each 1-km pixel, the input data consisted of texture, rock fraction, and percentages of sand, silt, and clay of 11 soil layers. Depth to bedrock was also included. Thus, depth could be obtained either from the depth to bedrock or by examining the 11 layers. We applied the same methods as of White and Nemani (2004) to produce soil texture and rooting depth from the STATSGO data for use as TOPS inputs. First, for each pixel, we extracted only those layers having a depth less than or equal to the

Table 3
Time-variable data sets used in this study.

Source	Parameter	Data source or method	Purpose
Ameriflux data	ET	–	Satellite-based ET
	Rad.	–	Satellite-based ET
Satellite-based data	LST	MOD11A2; Wan et al. (2002)	Satellite-based ET
	EVI	MOD13A2; Huete et al. (2002)	Satellite-based ET
	LAI/FPAR	MOD15A2; Myneni et al. (2002)	TOPS simulation
Meteorological data	Temp.	CPC/NCDC data	TOPS simulation
	Prec.	CPC data	TOPS simulation
	VPD	Campbell and Norman (1998)	TOPS simulation
	Rad.	Satellite-based (GCIP)	Satellite-based ET and& TOPS simulation

ET, Rad., LST, EVI, LAI, Temp., Prec., VPD refer to evapotranspiration, surface solar radiation, land surface temperature, enhanced vegetation index, leaf area index, temperature, precipitation, and vapor pressure deficit, respectively.

recorded depth to bedrock. For these layers, we then extracted, where available, the sand, silt, clay, and texture information. Next, we calculated the layer-weighted percentage of sand, silt, and clay information. Finally, we calculated the rock fraction-corrected layer-weighted soil depth. We used HYDRO1K data (http://edc.usgs.gov/products/elevation/gtopo30/hydro/index.html) for elevation data.

3. Experiment

The study consisted of two steps: point and spatial analysis for model simulation and evaluation. First, we tested the satellite-based ET, estimated rooting depth, and simulated ET seasonality at four flux sites in California. Second, we extended the analysis to all of California to estimate spatial patterns of rooting depth and seasonal ET variations. We also assessed the impacts of rooting depth refinements on simulated GPP. For all simulations, we used two different rooting depth settings: STATSGO (soil survey-based; Section 2.3.4) and optimized rooting depths (Section 2.2.3).

First, we tested the performance of the satellite data-based and model-based ET estimations at four flux sites in California. To do so, we tuned the SVM model using satellite-based EVI and LST, flux site-based radiation, and land cover as inputs, and we obtained ET as the output. Using the established model, we applied satellite-based data (LST, EVI, Rad, and LC) to obtain the continuous 8-day averaged ET from 2001 to 2006. The estimated ET and TOPS ecosystem models are used to infer the rooting depth at each flux site based on the algorithms described in Section 2.2.3. We then ran the model using STATSGO, optimized the rooting depth for model testing, and analyzed the impacts of different rooting depth settings on simulated ET seasonality. For the simulations, we ran the model from 1997 to 2006, and only the outputs from 2001 to 2003 were used for estimating rooting depth, and from 2004 to 2006 for model validation.

Second, we performed spatial analysis for California. We started by obtaining the spatio-temporal variations of ET based on the satellite-based ET estimation. Then, using the satellite-based ET and TOPS terrestrial ecosystem model, we estimated the rooting depth in each grid. Last, we ran the model using STATSGO and optimized rooting depths and analyzed the sensitivity of ET and GPP seasonality to the rooting depth settings. For the simulations, we ran the model from 1997 to 2006, and only the outputs from 2001 to 2003 were used for estimating rooting depth, and from 2004 to 2006 for model validation.

4. Results and discussion

4.1. Point analysis

4.1.1. Evaluation of satellite-based ET estimation

We used ET observations from 2000 to 2006 at 10 Ameriflux observation sites to develop the model; we thus obtained SVM kernel parameters of $C = 1.072$, $\sigma = 7.464$, and $\varepsilon = 0.203$, with a correlation coefficient of $R^2 = 0.76$ and a RMSE of 0.49 $mmH_2O\ day^{-1}$ between the observed and satellite-based ETs. Compared with Yang et al. (2006), we obtained a similar R^2-value but a smaller RMSE value, which was probably due to our model, which was more spatially specific than their original spatial scale.

Detailed evaluations of the satellite-based ET time variations revealed its promising capability to estimate spatio-temporal ET variations in the study area (Fig. 4). For example, at Blodgett Forest site, Vaira Ranch, and Tonzi Ranch, both seasonal and interannual ET variations were captured well by the satellite-based ET estimation with high R^2 and small RMSEs ($R^2 = 0.93$ and RMSE = 0.43 $mmH_2O\ day^{-1}$ for Blodgett Forest, $R^2 = 0.76$ and RMSE = 0.34 $mmH_2O\ day^{-1}$ for Tonzi Ranch, and $R^2 = 0.83$ and RMSE = 0.37 $mmH_2O\ day^{-1}$ for Vaira Ranch). In the dry open shrubland site of Sky Oaks, the accuracy of the model is lower than the other sites ($R^2 = 0.35$ and RMSE = 0.47 $mmH_2O\ day^{-1}$) due to small seasonal ET variation and difficulty in monitoring sparse vegetation cover from satellite-based observation (Sims et al., 2006).

4.1.2. Rooting depth estimation and its impacts on ET seasonality

Optimization of the rooting depth based on the satellite-based ET and the TOPS model estimates deeper rooting depths than STATSGO does, with smaller RMSEs between the satellite-based

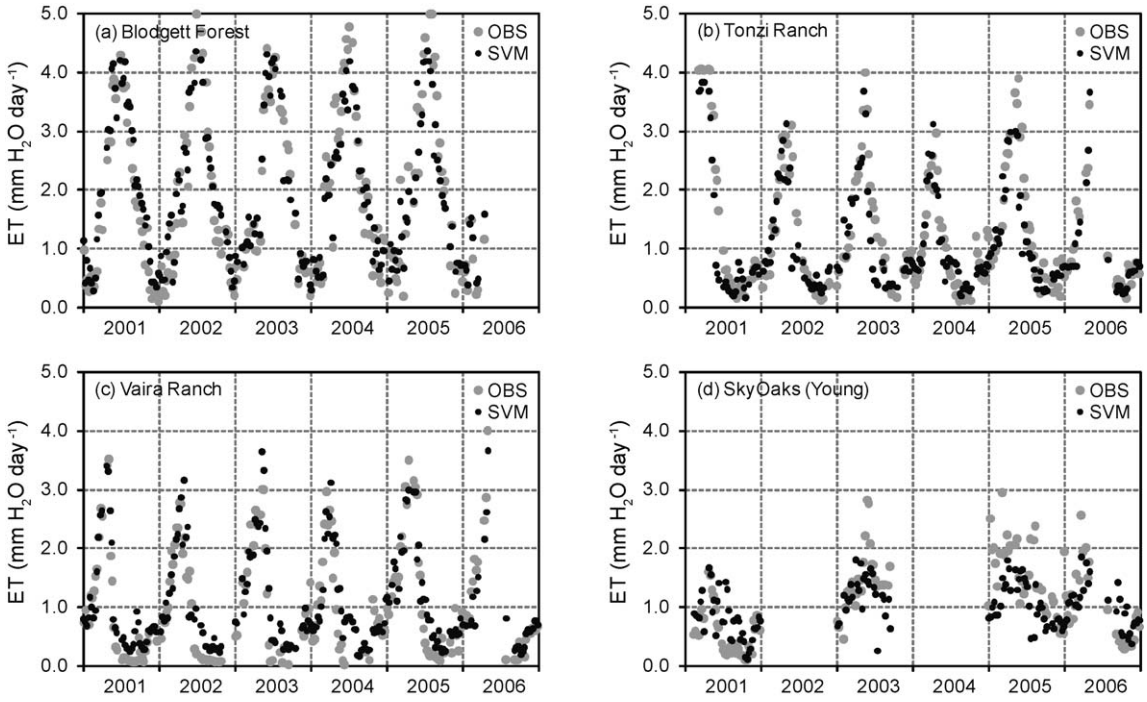

Fig. 4. Temporal variations in observed (gray) and satellite-based (black) evapotranspiration at four flux sites in California.

Table 4
Estimated and STATSGO rooting depths at flux sites, California.

Site	STATSGO	Optimized
Blodgett Forest	1.3 m (1.20)	3.9 m (0.43)
Tonzi Ranch	0.4 m (0.46)	0.7 m (0.32)
Vaira Ranch	0.4 m (0.42)	0.5 m (0.39)
Sky Oaks (Young)	0.4 m (0.54)	2.4 m (0.47)

Numbers in parentheses are the RMSE ($mmH_2O\ day^{-1}$) between satellite-based and simulated 8-day averaged ET from 2004 to 2006.

and model-based ETs (Table 4). Models based on optimized rooting depths successfully simulated ET seasonal variations, providing data that are consistent with satellite-based estimation and show small errors. Due to large differences between the optimized and STATSGO rooting depths, the improvement of the simulated ET seasonality at Blodgett Forest was drastic. For Vaira Ranch and Tonzi Ranch sites, although the differences between the optimized and STATSGO rooting depths were not as large, improvements in the seasonal ET simulations were still seen in the middle to end of the growing season. For Sky Oaks site, only slight improvements were achieved despite of deeper rooting depth estimation. It is probably due to difficulty in monitoring sparse vegetation using satellite-based vegetation index (Sims et al., 2006) and insufficient modeling of bare soil evaporation after rainy day (spikes detected in Fig. 5(d)).

Field observations also support that the estimated rooting depths are reasonable. For example, deep rooting depths have been reported for the Blodgett Forest site (at least 2 m; Laurent Misson, personal communications). In addition, 0.5 m of rooting depth is reported at Vaira Ranch site (Ryu et al., 2008).

The point-based analysis suggests the importance of rooting depth refinement in the ET simulations. The optimization processes produced more reasonable rooting depth and simulated ET estimations. From the results of the point-scale analysis, we expect spatial application of the method to significantly improve the seasonal ET simulations.

4.2. Spatial analysis

4.2.1. Rooting depth and impacts on ET

Spatial patterns of optimized rooting depth, as estimated from the satellite-based ET and TOPS ecosystem model, show very clear spatial variations that are dependent on vegetation type (Fig. 5). Deep rooting depths were estimated across the whole forest region in the northern part of California (3–5 m) and in some cropland regions of the central valley (>5 m), whereas most of the southern regions show shallow rooting depths. The forest regions are generally characterized by dry summers with high ET (e.g., Figs. 2 and 4); therefore, deep rooting systems are required to sustain peak ET in the summer, as shown in the point analysis. The central valley is basically irrigated cropland; because our model does not include irrigation effects, the deeper rooting depths are estimated to sustain high ET during the summer, which is enabled by the water supply from irrigation.

Compared to the STATSGO-based rooting depth estimations, our estimated rooting depths are much deeper in the northern forests and the central valley cropland regions (Fig. 6). For example, the STATSGO-based rooting depth is around 1 m throughout the forest regions, whereas this study estimated them to be at least 2–3 times deeper. We also found that estimated rooting depth in northern forests are much deeper than that from literature (e.g., 1.04 m based on the depth of 95% root biomass for warm-temperate forest and 1.71 m based on the depth of 95% root biomass for Mediterranean shrubland and woodland; Schenk and Jackson, 2002), and close to its maximum (3.9 ± 0.4 m for temperate coniferous forest; Canadell et al., 1996).

The choice of rooting depth settings significantly affect the RMSEs between the modeled and satellite-based ET values, and the optimized rooting depth improved the model performance in terms of ET seasonality (Fig. 7). Compared with the simulation based on STATSGO rooting depths, we found that RMSEs decreased significantly wherever estimated rooting depths were significantly deeper than the STATSGO-based survey values. For example, the

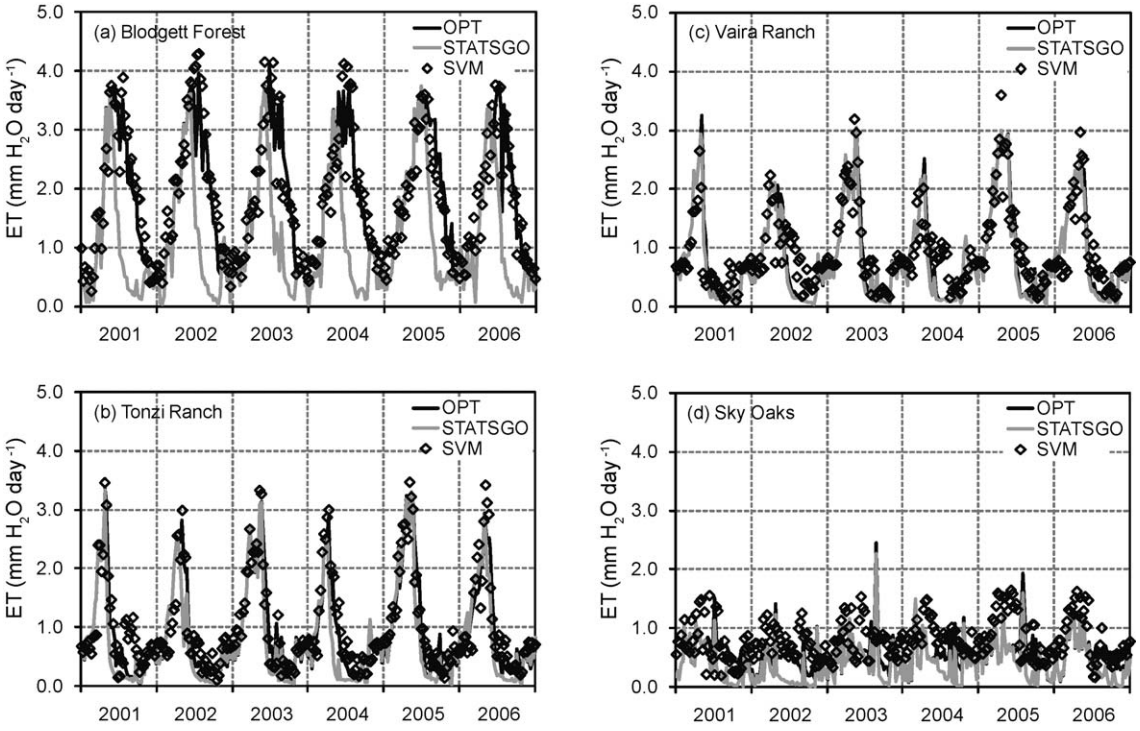

Fig. 5. Model-simulated (based on optimized (black line) and STATSGO rooting depths (gray)) and satellite-based (diamond) ET variations from 2001 to 2006. Years 2001–2003 and 2004–2006 are used for model parameter derivation and validation, respectively.

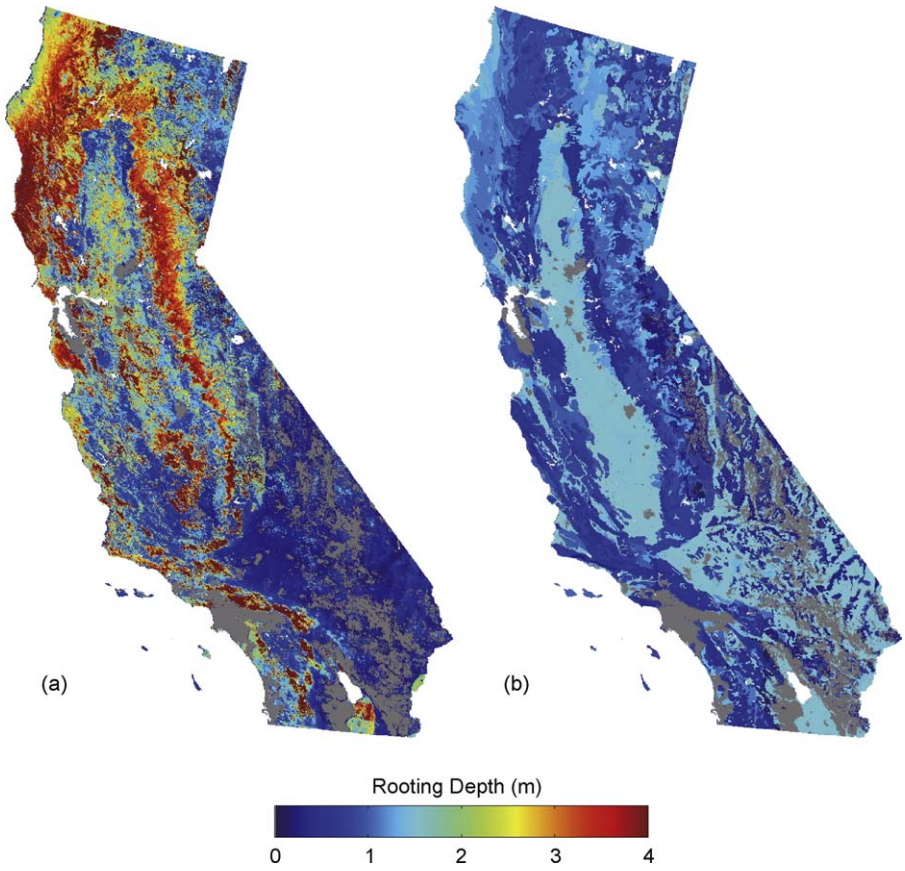

Fig. 6. Spatial patterns in (a) optimized and (b) STATSGO rooting depths in California. Barren and urban areas are shown in gray.

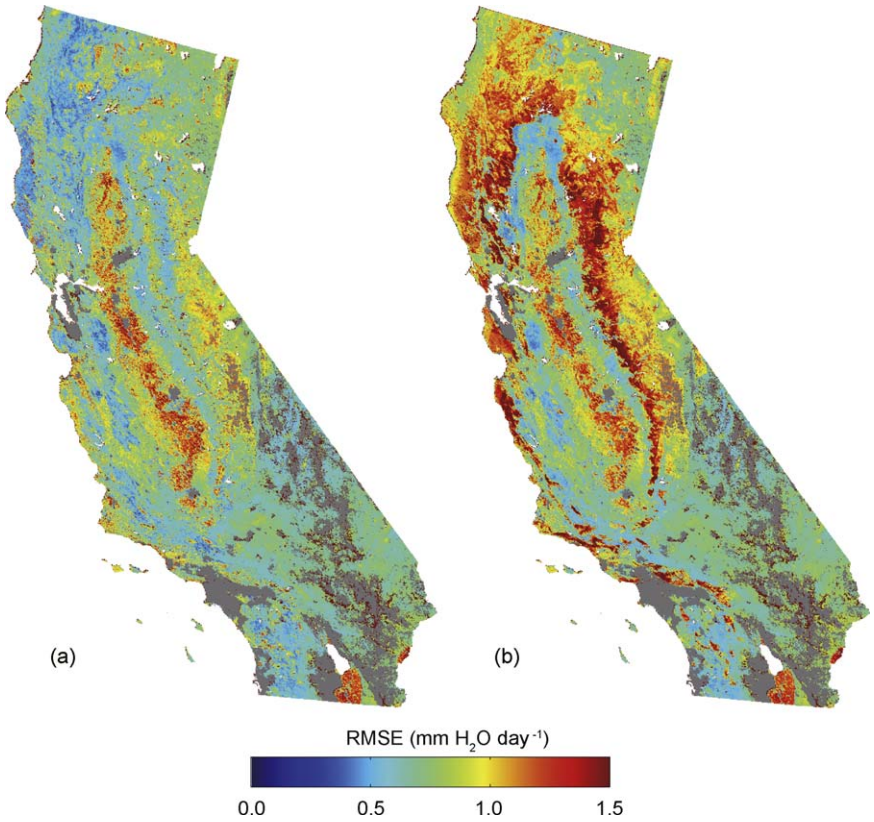

Fig. 7. Root mean square error of 8-day ET variations obtained by TOPS under (a) optimized and (b) STATSGO rooting depth settings and satellite-based ones. Three years of results are used, from 2004 to 2006. Barren and urban areas are shown in gray.

large RMSEs based on the STATSGO rooting depth settings across all the forest regions (>1.2 mmH_2O day^{-1}) are greatly improved in our simulation based on optimized rooting depth (<0.8 mmH_2O day^{-1}).

Averaging the rooting depths in each land cover class shows the strong contrast among land cover classes in estimated rooting depths (Table 5). Evergreen needle-leaf forests have the deepest rooting depths (3.1 ± 1.2 m), with Savanna classes also showing great depths (>2.0 m). The rooting depth refinement also drastically improved ET estimation in evergreen needle-leaf forest regions, leading to a 40% reduction in the RMSE between satellite-based and model-based ET values. Improvements in ET estimations are also seen for other land cover classes, although none as drastic as evergreen needle-leaf forests.

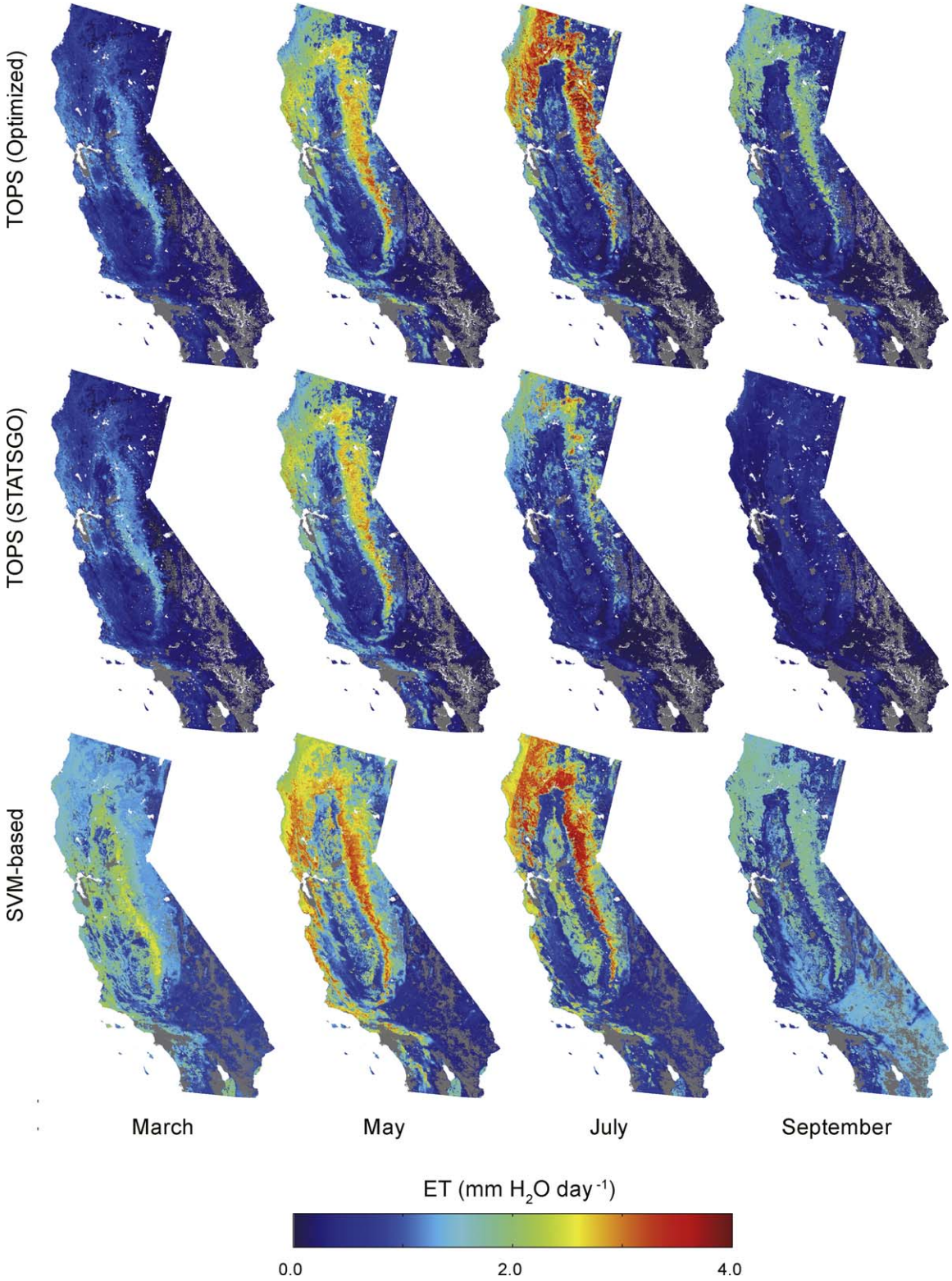

Fig. 8. Seasonal ET variations in TOPS under optimized rooting depth (top), and TOPS under STATSGO rooting depths (middle), and SVM-based estimations (bottom). Results from March, May, July, and September are shown by averaging three years of data, from 2004 to 2006. Barren and urban areas are shown in gray.

Table 5
Estimated and STATSGO rooting depths (m) and RMSEs between satellite-based and model-based ET ($mmH_2O\ day^{-1}$) in each land cover class.

Land cover	Estimated rooting depth (RMSE)	STATSGO rooting depth (RMSE)
Evergreen needle-leaf forest	3.3 ± 1.4 m (0.66)	0.9 ± 0.3 m (1.10)
Open shrubland	0.6 ± 0.5 m (0.73)	1.0 ± 0.5 m (0.73)
Woody Savanna	2.2 ± 1.7 m (0.67)	0.8 ± 0.4 m (0.80)
Savanna	2.2 ± 1.4 m (0.74)	1.0 ± 0.4 m (0.78)
Grassland	1.3 ± 1.0 m (0.79)	0.9 ± 0.5 m (0.80)
Cropland	2.4 ± 1.3 m (1.02)	1.4 ± 0.1 m (1.02)

RMSEs are calculated using 2004–2006 satellite-based and simulated 8-day averaged ET.
Only the land cover classes cover over 20,000 km^2 are selected.

Monthly variations in the simulated and satellite-based ETs show that the simulation based on optimized rooting depth agrees very well with the satellite-based ET; however, the simulation based on the STATSGO rooting depth underestimated the summer ET in forest regions (Fig. 8). The seasonal variations in satellite-based ET show increases in ET from spring to summer, with peaks in July. The simulated ET based on optimized rooting depth shows the same seasonal evolution in the northern forest regions; however, the simulation based on the STATSGO rooting depth shows a large decline after July. The sufficient soil water holding capability that comes with deeper rooting depths improved the model significantly.

4.2.2. Impacts on simulated GPP seasonality

Due to tightly coupled effects of ET and GPP, optimization of rooting depth affects the simulated GPP seasonality similar to the way ET does, especially in the summer, and annual total GPP was greatly increased (50–100%) in the forest regions by the refinement of rooting depth (Fig. 9). In the STATSGO rooting depth simulation, summer GPP values are underestimated due to insufficient water availability with the shallow rooting depths in the forest regions. In contrast, the model based on optimized rooting depth simulated a higher GPP in summer that was consistent with the satellite-based ET seasonality. This increased annual GPP value in the forest regions and some coastal regions resulted in improved carbon cycle simulations. In most grassland and shrubland regions, significant changes in annual GPP were not detected due to the difficulty of interpreting satellite observations of sparse vegetation (see Sections 4.1.1 and 4.1.2), and/or shallow rooting depths in these ecosystems as found from the soil survey.

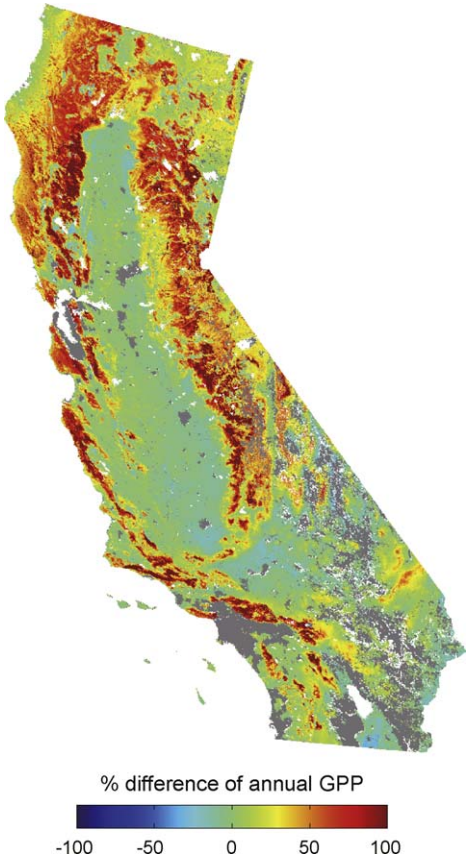

Fig. 9. Percentage difference of annual GPP between simulations with STATSGO rooting depth and optimized rooting depth, calculated as 100 × (optimized–STATSGO)/STATSGO. Annual GPP is calculated from the 2004 to 2006 average. Barren and urban areas are shown in gray.

4.3. Model limitation and further improvements

Although the rooting depth optimization process improved the spatial patterns of rooting depths and water and carbon cycle simulations in California, potential limitations and further improvements should be noted.

First, the eddy covariance's estimate of ET contains errors due to the problems of energy imbalance. The quantity, ET + H (sensible heat), measured by eddy covariance is often less than the quantity, R_n (net radiation) − G (ground heat flux) (Wilson et al., 2002; Foken, 2008). Although this imbalance potentially affects observed ET, satellite-based ET estimation and rooting depth refinement, our findings of deep rooting depth over evergreen needle-leaf forest regions in California are not substantially affected.

Second, the assumption of a one-box soil water layer in TOPS tends to overestimate the soil water evaporation, underestimate the runoff due to ignoring vertical water transport, and underestimate the water stress for stomatal conductance due to the lack of vertical distribution of water and roots. However, these effects are not important in this study because (1) the potential overestimation of soil water evaporation due to a single soil water layer does not have a large impact in dense forests, (2) because runoff occurs mostly in the rainy season, the impact on our rooting depth estimation is small because it is largely determined by the amount of precipitation and the length of the dry season, and (3) underestimation of the water stress for stomatal conductance and GPP due to the lack of vertical distribution of water and roots may be partially compensated for by hydraulic redistribution (Candwell et al., 1998; Brooks et al., 2002). In addition, the credibility of estimated rooting depth and modeled ET are guaranteed by validations at the flux sites.

Third, the current water cycle model ignores the lateral water flow due to topography and potentially overestimates vegetation water stress and rooting depths. However, our method estimated appropriate rooting depths that were consistent with ground observations, and it greatly improved the simulated ET seasonality. We therefore conclude that these effects will not substantially affect the rooting depth estimation or model accuracy.

Fourth, a lack of irrigation effects on the water cycle model led to an estimation of deeper rooting depth in the central valley cropland regions. Development of an irrigation module is required

for accurate modeling of water stress in these regions. Currently, the model results supply the amount of water that would be required to support vegetation growth during the growing seasons.

5. Conclusion

In this study, we estimated rooting depths in California using satellite-based ET and an ecosystem model by minimizing differences between the model-based and satellite-based ET values and then analyzing the impacts on the accuracy of the simulated ET seasonality. Large differences were found between the optimized and soil survey (STATSGO)-based rooting depths in the northern forest regions. In these areas, the significantly deeper rooting depths (>3 m) estimated in the study were able to successfully reproduce the satellite-based ET seasonality with a peak in the summer, whereas the shallow rooting depths based on STATSGO (<1.5 m) could not sustain high ETs in summer. Over the grass and shrub regions in central and southern California, estimated rooting depths were similar to those reported by STATSGO, probably due to the shallow rooting depths in these ecosystems. Our analysis suggests that accurately estimating rooting depth is important for ecosystem modeling and that satellite-based data can help to constrain the spatial variability of rooting depths to improve water and carbon cycle modeling.

This study has two potential implications for the use of satellite-based data in terrestrial ecosystem modeling. First, we showed an example of the powerful application of satellite-based products to improve a terrestrial biosphere model. The satellite-based products that are independent of the model are useful in constraining the ecosystem models, as was also shown by Yang et al. (2007). Second, refinement of the water cycle model in this study also improved carbon cycle modeling, illustrating that improving the water cycle model is an important step for accurate carbon cycle modeling. Especially for seasonally dry forest environments (e.g., Baker et al., 2008; Ichii et al., 2007; Tanaka et al., 2004), improved estimation of rooting depth will substantially increase estimated GPP.

Acknowledgements

This research was supported by funding from NASA's Science Mission Directorate through EOS (K. Ichii, W. Wang, H. Hashimoto, R.R. Nemani) and Grand-in-Aid for Scientific Research (C) (ID: 50345865) by Japan Society for the Promotion of Science (K. Ichii). Flux tower measurements were funded by the Department of Energy, the National Oceanic and Atmospheric Administration, the National Aeronautics and Space Administration (NASA), and the National Science Foundation. Special thanks to all the scientists and support teams at the flux towers.

References

Alfaro, E.J., Gershunov, A., Cayan, D., 2006. Prediction of summer maximum and minimum temperature over the central and western United States: the roles of soil moisture and sea surface temperature. J. Clim. 16, 1407–1421.

Andren, O., Paustian, K., 1987. Barley straw decomposition in the field: a comparison of models. Ecology 68, 1190–1200.

Baker, I.T., Prihodko, L., Denning, A.S., Goulden, M., Miller, S., da Rocha, H.R., 2008. Seasonal drought stress in the Amazon: reconciling models and observations. J. Geophys. Res. 113, G00B01, doi:10.1029/2007JG000644.

Baldocchi, D.D., Xu, L.K., Kiang, N., 2004. How plant functional-type, weather, seasonal drought, and soil physical properties alter water and energy fluxes of an oak-grass Savanna and an annual grassland. Agric. Forest Meteorol. 123, 13–39.

Ball, J.T., Woodrow, I.E., Berry, J.A., 1987. A model predicting stomatal conductance and its contribution to the control of photosynthesis under different environmental conditions. In: Biggins, J. (Ed.), Progress in Photosynthesis Research, vol. 4. M. Nijhoff Publishers, Dordrecht, pp. 221–224.

Brooks, J.R., Meinzer, F.C., Coulombe, R., Gregg, J., 2002. Hydraulic redistribution of soil water during summer drought in two contrasting Pacific Northwest coniferous forests. Tree Physiol. 22, 1107–1117.

Buermann, W., Dong, J., Zeng, X., Dickinson, R.E., 2001. Evaluation of the utility of satellite-based vegetation leaf area index data for climate simulations. J. Clim. 14, 3536–3550.

Campbell, G.S., Norman, J.M., 1998. Environmental Biophysics. Springer-Verlag, New York.

Canadell, J., Jackson, R.B., Ehleringer, J.B., Mooney, H.A., Sala, O.E., Schulze, E.D., 1996. Maximum rooting depth of vegetation types at the global scale. Oecologia 108, 583–595.

Candwell, M.M., Dawson, T.E., Richards, J.H., 1998. Hydraulic lift: consequences of water efflux from the roots of plants. Oecologia 113, 151–161.

Cook, R.B., Margle, S.M., Holladay, S.K., Heinsch, F.A., Schaaf, C.B., 2004. Subsets of remote sensing products for Ameriflux sites: MODIS ASCII subsets. Ameriflux Annual Meeting.

Cristianini, N., Shawe-Taylor, J., 2000. An introduction to support vector machines and other kernel-based learning methods. Cambridge University Press, Cambridge, UK.

Foken, T., 2008. The energy balance closure problem: an overview. Ecol. Appl. 18, 1351–1367.

Friedl, M.A., McIver, D.K., Hodges, J.C.F., Zhang, X.Y., Muchoney, D., Strahler, A.H., Woodcook, C.E., Gopal, S., Schneider, A., Cooper, A., Baccini, A., Gao, F., Schaaf, C., 2002. Global land cover mapping from MODIS: algorithms and early results. Remote Sens. Environ. 83, 287–302.

Goldstein, A.H., Hultman, N.E., Fracheboud, J.M., Bauer, M.R., Panek, J.A., Xu, M., Qi, Y., Guenther, A.B., Baugh, W., 2000. Effects of climate variability on the carbon dioxide, water, and sensible heat fluxes above a ponderosa pine plantation in the Sierra Nevada (CA). Agric. Forest Meteorol. 101, 113–129.

Guswa, A.J., Celia, M.A., Rodrigurz-Iturbe, I., 2002. Models of soil moisture dynamics in ecohydrology: A comparative study. Water Resour. Res. 38 (9), 1166, doi:10.1029/2001WR000826.

Huang, J., van den Dool, H.M., Georgakakos, K.P., 1996. Analysis of model-calculated soil moisture over the United States (1931–1993) and applications to long-range temperature forecasts. J. Clim. 9, 1350–1362.

Huete, A., Didan, K., Miura, T., Rodriguez, E., 2002. Overview of the radiometric and biophysical performance of the MODIS vegetation indices. Remote Sens. Environ. 83, 195–213.

Ichii, K., Hashimoto, H., White, M.A., Potter, C.S., Hutyra, L.R., Huete, A.R., Myneni, R.B., Nemani, R.R., 2007. Constraining rooting depths in tropical rainforests using satellite data and ecosystem modeling for accurate simulation of GPP seasonality. Global Change Biol. 13, 67–77.

Ichii, K., White, M.A., Votava, P., Michaelis, A., Nemani, R.R., 2008. Evaluation of snow models in terrestrial biosphere models using ground observation and satellite data: impact on terrestrial ecosystem processes. Hydrol. Process. 22, 347–355.

Jolly, W.M., Graham, J.M., Michaelis, A., Nemani, R.R., Running, S.W., 2005. A flexible, integrated system for generating meteorological surfaces derived from point sources across multiple geographic scales. Environ. Model. Software 20 (7), 873–882.

Kleidon, A., 2004. Global datasets of rooting zone depth inferred from inverse methods. J. Clim. 17, 2714–2722.

Kleidon, A., Heimann, M., 1998. A method of determining rooting depth from a terrestrial biosphere model and its impacts on the global water and carbon cycle. Global Change Biol. 4, 275–286.

Koster, R.D., Dirmeyer, P.A., Guo, Z., Bonan, G., Chan, E., Cox, P., Gordon, C.T., Kanae, S., Kowalczyk, E., Lawrence, D., Liu, P., Lu, C.H., Malyshev, S., McAvaney, B., Mitchell, K., Mocko, D., Oki, T., Oleson, K., Verseghy, D., Vasic, R., Xue, Y., Yamada, T., 2004. Regions of strong coupling between soil moisture and precipitation. Science 305, 1138–1140.

Lathrop Jr., R.G., Aber, J.D., Bognar, J.A., 1995. Spatial variability of digital soil maps and its impact on regional ecosystem modeling. Ecol. Modell. 82, 1–10.

Law, B.E., Turner, D., Campbell, J., Sun, O.J., Tuyl, S.V., Ritts, W.D., Cohen, W.B., 2004. Disturbance and climate effects on carbon stocks and fluxes across Western Oregon USA. Global Change Biol. 10, 1429–1444.

Lipson, D.A., Wilson, R.F., Oechel, W.C., 2005. Effects of elevated atmospheric CO_2 on soil microbial biomass, activity, and diversity in a chaparral ecosystem. Appl. Environ. Microbiol. 71, 8573–8580.

Miller, D.A., White, R.A., 1998. A conterminous United States multilayer soil characteristics data set for regional climate and hydrology modeling. Earth Interact. 2, 1–13.

Misson, L., Tu, K.P., Boniello, B., Goldstein, A.H., 2006. Seasonality of photosynthetic parameters in a multi-specific and vertically complex forest ecosystem in the Sierra Nevada California. Tree Physiol. 26, 729–741.

Monteith, J.L., 1972. Solar radiation and productivity in tropical ecosystems. J. Appl. Ecol. 9, 747–766.

Myneni, R.B., Hoffman, S., Knyazikhim, Y., Privette, J.L., Glassy, J., Tian, Y., Wang, Y., Song, X., Zhang, Y., Smith, Y., Lotsch, A., Friedl, M., Morisette, J.T., Votava, P., Nemani, R.R., Running, S.W., 2002. Global products of vegetation leaf area and fraction absorbed PAR from year one of MODIS data. Remote Sens. Environ. 83, 214–231.

Nemani, R., White, M., Thornton, P., Nishida, K., Reddy, S., Jenkins, J., Running, S.W., 2002. Recent trends in hydrologic balance have enhanced the terrestrial carbon sink in the United States. Geophys. Res. Lett. 29 (10), doi:10.1029/2002GL014867.

Nemani, R.R., White, M.A., Pierce, L., Votava, P., Coughlan, J., Running, S.W., 2003. Biospheric monitoring and ecological forecasting. Earth Obs. Mag. 12, 6–8.
Nemani, R.R., Hashimoto, H., Votava, P., Melton, F., Wang, W., Michaelis, A., Mutch, L., Milesi, C., Hiatt, S., White, M., 2009. Monitoring and forecasting ecosystem dynamics using the Terrestrial Observation and Prediction System (TOPS). Remote Sens. Environ. 113, 1497–1509.
Nepstad, D.C., Carvalho, C.R.D., Davidson, E.A., Jipp, P.H., Lefebvre, P.A., Negreiros, G.H., Silva, E.D.D., Stone, T.A., Trumbore, S.E., Vieira, S., 1994. The role of deep roots in the hydrological and carbon cycles of Amazonian forests and pastures. Nature 372, 666–669.
Nishida, K., Nemani, R.R., Running, S.W., Glassy, J.M., 2003. An operational remote sensing algorithm of land surface evaporation. J. Geophys. Res. 108 (D9), 4270, doi:10.1029/2002JD002062.
Pinker, R.T., Laszlo, O., Tarpley, J.D., Mitchell, K., 2002. Geostationary satellite parameters for surface energy balance. Adv. Space Res. 30, 2427–2432.
Potter, C.S., Randerson, J.T., Field, C.B., Matson, P.A., Vitousek, P.M., Mooney, H.A., Klooster, S.A., 1993. Terrestrial ecosystem production: a process model based on global satellite and surface data. Global Biogeochem. Cycles 7, 785–809.
Press, W.H., Flannery, B.P., Teukolsky, S.A., Vetterling, W.T., 1992. Golden section search in one dimension. 2nd edition. Numerical Recipes in C: The Art of Scientific Computing, 2nd edition, Cambridge University Press, Cambridge, pp. 397–401 (chapter 10.1).
Rawlins, M.A., Frolking, S., Lammers, R.B., Vörösmarty, C.J., 2006. Effects of uncertainty in climate inputs on simulated evapotranspiration and runoff in the Western Arctic. Earth Interact. 10 (18), 1–18.
Ryu, Y., Baldocchi, D.D., Ma, S., Hehn, T., 2008. Interannual variability of evapotranspiration and energy exchange over an annual grassland in California. J. Geophys. Res. 113, D09104, doi:10.1029/2007JD009263.
Schenk, H.J., Jackson, R.B., 2002. The global biogeography of roots. Ecol. Monogr. 72, 311–328.
Schenk, H.J., Jackson, R.B., 2005. Mapping the global distribution of deep roots in relation to climate and soil characteristics. Geoderma 126, 129–140.
Shaw, D.C., Franklin, J.F., Bible, K., Klopatek, J., Freeman, E., Greene, S., Parker, G.G., 2004. Ecological setting of the wind river old-growth forest. Ecosystems 7, 427–439.
Sims, D.A., Luo, H., Hastings, S., Oechel, W., Rahman, A.F., Gamon, J.A., 2006. Potential adjustments in vegetation greenness and ecosystem CO_2 exchange in response to drought in a Southern California chaparral ecosystem. Remote Sens. Environ. 103, 289–303.
Sitch, S., Smith, B., Prentice, I.C., Arneth, A., Bondeau, A., Cramer, W., Kaplan, J., Levis, S., Lucht, W., Sykes, M., Thonicke, K., Vanevski, S., 2003. Evaluation of ecosystem dynamics, plant geography, and terrestrial carbon cycling in the LPJ dynamic vegetation model. Global Change Biol. 9, 161–185.
Stewart, J.B., 1988. Modelling surface conductance of pine forest. Agr. Forest Meteorol. 43, 19–35.
Stylinski, C.D., Gamon, J.A., Oechel, W.C., 2002. Seasonal patterns of reflectance indices, carotenoid pigments and photosynthesis of evergreen chaparral species. Oecologia 131, 366–374.
Tanaka, K., Takizawa, H., Kume, T., Xu, J., Tantasirin, C., Suzuki, M., 2004. Impact of rooting depth and soil hydraulic properties on the transpiration peak of an evergreen forest in northern Thailand in the late dry season. J. Geophys. Res. 109, D23107, doi:10.1029/2004JD004865.
Thornton, P.E., 1998. Regional ecosystem simulation: combining surface- and satellite-based observations to study linkages between terrestrial energy and mass budgets. PhD Thesis. The University of Montana, Missoula.
Thornton, P.E., Law, B.E., Gholz, H.L., Clark, K.L., Falge, E., Ellsworth, D.S., Goldstein, A.H., Monson, R.K., Hallinger, D., Falk, M., Chen, J., Sparks, J.P., 2002. Modeling and measuring the effects of disturbance history and climate on carbon and water budgets in evergreen needleleaf forests. Agr. Forest Meteorol. 113, 185–222.
Vapnik, V.N., 1998. Statistical Learning Theory. Wiley, New York.
Wan, Z., Zhang, Y., Zhang, Q., Li, Z., 2002. Validation of the land-surface tempearture products retrieved from Terra Moderate Resolution Imaging Spectroradiometer data. Remote Sens. Environ. 83, 163–180.
White, M.A., Nemani, R.R., 2004. Soil water forecasting in the continental United States: relative forcing by meteorology versus leaf area index and the effects of meteorological forecast errors. Can. J. Remote Sens. 30, 717–730.
White, M.A., Thornton, P.E., Running, S.W., Nemani, R.R., 2000. Parameterization and sensitivity analysis of the BIOME-BGC terrestrial ecosystem process model: net primary production controls. Earth Interact. 4 (3), 1–85.
Wilson, K., Goldstein, A., Falge, E., Aubinet, M., Baldocchi, D., Berbigier, P., Bernhofer, C., Ceulemans, R., Dolman, H., Field, C., Grelle, A., Ibrom, A., Law, B.E., Kowalski, A., Meyers, T., Moncrieff, J., Monson, Russ, Oechel, W., Tenhunen, J., Valentini, R., Verma, S., 2002. Energy balance closure at FLUXNET sites. Agric. Forest Meteorol. 113, 223–243.
Yang, F., Ichii, K., White, M.A., Hashimoto, H., Michaelis, A.R., Votava, P., Zhu, A.X., Huete, A., Running, S., Nemani, R.R., 2007. Developing a continental-scale measure of gross primary production by combining MODIS and Ameriflux data through support vector machine. Remote Sens. Environ. 110, 109–122.
Yang, F., Kumar, A., Lau, K.M., 2004. Potential predictability of U.S. summer climate with "perfect" soil moisture. J. Hydromet. 5, 883–895.
Yang, F., White, M., Michaelis, A., Ichii, K., Hashimoto, H., Votava, P., Zhu, A.X., Nemani, R.R., 2006. Prediction of continental scale evapotranspiration by combining MODIS and AmeriFlux data through Support Vector Machine. IEEE Trans. Geosci. Remote Sens. 44, 3452–3461.
Zhang, Y., Wegehenkel, M., 2006. Integration of MODIS data into a simple model for the spatial distributed simulation of soil water content and evapotranspiration. Remote Sens. Environ. 104, 393–408.
Zhu, J., Liang, X.Z., 2005. Regional climate model simulation of U.S. soil temperature and moisture during 1982–2002. J. Geophys. Res. 110, D24110, doi:10.1029/2005JD006472.